Received: 12 February 2019 | Revised: 5 June 2019 | Accepted: 11 December 2019
DOI: 10.1002/we.2475

WILEY

RESEARCH ARTICLE

Structural load mitigation control for wind turbines: A new performance measure

M. Hung Do[1] | Jackson G. Njiri[2] | Dirk Söffker[1]

[1]Chair of Dynamics and Control, University of Duisburg-Essen, Duisburg, Germany
[2]Department of Mechatronics Engineering, Jomo Kenyatta University of Agriculture and Technology, Juja, Kenya

Correspondence
M. Hung Do, Chair of Dynamics and Control, University of Duisburg-Essen, Duisburg 47057, Germany.
Email:hung.do@uni-due.de

Present Address:
Hung M. Do, Lotharstr. 1, Duisburg 47057, Germany

Funding information
Vietnam International Education Development (VIED) scholarship

Summary

Structural loads of wind turbines are becoming critical because of the growing size of wind turbines in combination with the required dynamic output demands. Wind turbine tower and blades are therefore affected by structural loads. To mitigate the loads while maintaining other desired conditions such as the optimization of power generated or the regulation of rotor speed, advanced control schemes have been developed during the last decade. However, conflict and trade-off between structural load reduction capacity of the controllers and other goals arise; when trying to reduce the structural loads, the power production or regulation performance may be also reduced. Suitable measures are needed when designing controllers to evaluate the control performance with respect to the conflicting control goals. Existing measures for structural loads only consider the loads without referring to the relationship between loads and other control performance aspects. In this contribution, the conflicts are clearly defined and expressed to evaluate the effectiveness of control methods by introducing novel measures. New measures considering structural loads, power production, and regulation to prove the control performance and to formulate criteria for controller design are proposed. The proposed measures allow graphical illustration and numerical criteria describing conflicting control goals and the relationship between goals. Two control approaches for wind turbines, PI and observer-based state feedback, are defined and used to illustrate and to compare the newly introduced measures. The results are obtained by simulation using Fatigue, Aerodynamics, Structures, and Turbulence (FAST) tool, developed by the National Renewable Energy Laboratory (NREL), USA.

KEYWORDS

advanced control, performance measure, structural load, wind turbine

1 | INTRODUCTION

The growing concern about environmental issues and the exhausting of traditional fossil fuels lead to the need for alternative environmentally friendly energy sources. Among developing sustainable energy, wind energy is currently one of the most effective and fastest growing sources of electricity. A typical method to harvest wind energy is using wind turbines to convert wind kinetic energy to electric energy. To meet the growing demands on capacity and economic efficiency, wind turbines are being scaled up in size and using lightweight materials, thus increasing the flexibility and structural loads that wind turbines have to withstand.

Structural loads affecting tower, blades, and drivetrain mainly result from gravity and wind forces affecting the wind turbine rotor area. The wind speed changes stochastically in both direction and magnitude. The speed is usually larger at the upper part and lower at the bottom part of the turbine because of the wind shear, leading to unbalanced aerodynamic loads causing structural loads. Gyroscopic effects that arise from rotor rotation also induce structural loads. Gyroscopic forces yield cyclic stresses to the drivetrain and the blades resulting in fatigue loads.[1] These

The peer review history for this article is available at https://publons.com/publon/10.1002/we.2475

effects are stronger when the turbine sizes become larger leading to the increase in structural loads. The reduction of such periodic loads could reduce the operating cost and increase the wind turbines expected lifetime, which would lower the cost of wind energy.

Most large-scale wind turbines nowadays are characterized by variable-pitch and variable-speed control to maximize the energy extracted. The turbine rotor speed is controlled to track the optimal speed in region II (underrated wind speed) and to regulate the rotor speed at a rated value in region III (above-rated wind speed) by adjusting the generator torque and the pitch angle of blades.[2] Classical proportional-integral (PI) collective pitch control (CPC) controllers only regulate the rotor without considering structural loads. In modern large-scale wind turbines, structural loads such as tower vibration and drivetrain torsional vibration are reduced by using additional control loops for active damping at resonant frequencies.[3,4] Because of the strong coupling between control modes, special attention is required when designing control loops individually for different goals to avoid performance deterioration or unstabilizing the closed-loop system. To deal with the decoupling problem of single-input and single-output (SISO) approaches, advanced multiple-input and multiple-output (MIMO) controllers have been developed by wind energy researchers in order to realize multiple objectives such as regulating the rotor speed and mitigating structural loads at the same time. In Pintea et al[5] and Imran et al,[6] linear-quadratic-Gaussian (LQG) approach is used to calculate an optimal controller for speed regulation and blades and tower loads alleviation. Model predictive control (MPC) is commonly used for load reduction because of the ability to deal with constraints.[7] In Mirzaei et al,[8] a light detection and ranging (LIDAR) sensor is used to provide wind speed disturbance information in combination with MPC. The effects of wind variation on wind turbines can be mitigated by disturbance-accommodating control (DAC). The method uses a predefined disturbance model to estimate the wind speed as unknown disturbances. The blade flapwise bending moment is mitigated while regulating constant rotor speed thanks to the DAC independent pitch controller.[9] To reduce the drivetrain and tower loads and control the generator speed, in De Corcuera et al,[10] two robust H_∞ controllers are used for torque and pitch control. The simulation results show that the H_∞ controllers provide better performance than classical control approaches. In Yuan and Tang,[11] direct model reference adaptive control (DMRAC) is proposed to consider the varying wind speed and model uncertainties. The trade-off between generator speed regulation and load mitigation effect can be adjusted by modifying the weighting matrices of the adaptive laws. Both energy capture and fatigue loads are considered in Ma et al.[12] An algorithm to avoid tower resonance operating frequency is developed to mitigate the tower loads. The trade-off between power production and structural loads is considered by designing the parameter of an internal PI controller. In Xiao et al,[13] structural loads are taken into account by maximizing power using modified objective function of the extremum-seeking control (ESC) method. In general, the wind speed varies with height leading to unbalance forces that each turbine blade has to withstand. To reduce these asymmetrical loads, individual pitch control (IPC) is widely used.[3,14] Instead of using collective pitch for all blades, IPC controls each blade pitch individually. The core idea of IPC is to transform the blades rotating coordinate to a fixed frame by multi-blade coordinate transformation (MBC).[15] Controllers can be designed in the fixed frame by the above-mentioned methods; the control outputs then are converted back to rotating coordinate by the inverse transformation to produce individual pitch commands. Among modern control approaches, IPC full-state feedback (FSF) controls combined with observers are proved to have potential in load reduction by field tests on a real turbine.[16]

The main objectives of wind turbine control systems are to maximize the energy extracted from the wind, to minimize structural loads, and to guarantee system safety. The structural loads including blade bending moment and tower bending moment can be reduced by controlling the blade pitch angles collectively or individually with a proper algorithm. The challenge is that while trying to mitigate structural loads by modifying blade angles, the rotor speed will be affected, leading to performance degradation resulting in conflicts between structural loads mitigation and power control. The conflicts differ in different operating regions of wind turbines. When the wind speed is under the rated value that is defined as region II, the main control goal here is to maximize the generated power. The trade-off needs to be optimized in this region that is between energy efficiency and structural loads. To keep the wind turbine operating under safety limits in region III, the rotor/generator speed is kept constant at the rated value. Now, a compromise between speed regulation performance and loads reduction arises. To define an optimal compromise, complete knowledge about various elements affecting control performance is required. In addition, the contribution of each aspect to the addressed conflicting objectives such as load mitigation, speed regulation, and energy maximization needs to be evaluated by suitable measures.

In mentioned literature, to evaluate and compare the loads mitigation performances of control algorithms for wind turbines, power spectral density (PSD)[17] based on Fourier transform and damage equivalent load (DEL)[18] is commonly used. The methods use time-series historical data of blades and tower bending moment to calculate the strength of structural loads that the wind turbine has to withstand. The metric PSD analysis can calculate the strength of blades or tower variation at certain frequencies, which can generally describe the structural loads. On the other hand, DEL relates the cumulative fatigue damage representing the structural loads over a period of time. The metrics PSD and DEL only consider loads without referring to other goals, and the relationship between them makes it difficult to evaluate the overall performance including power production or rotor speed regulation criteria. The mentioned metrics need to be used in combination with other performance metrics to assess and design multi-objective controllers for wind turbines.

This contribution proposes novel measures based on time-series historical data obtained from wind turbines, such as blades/tower bending moments and rotor/generator speed, and the covariance of the data to assess the overall control performance of a wind turbine. The proposed measures can represent multi-control performances in a graph avoiding using separate metrics in designing controllers. A new parameter that defines the relation between control goals is introduced, which introduces a new measure for controller assessment and design. The measures are able to express multi-control objectives graphically and also in combination with related mathematical values. These illustrations give control engineers and control designers quantitative and qualitative insights into control performance criteria, enabling designers to modify control

parameters to reach desired result. The usages of the new measures are illustrated by comparing and tuning two commonly applied control approaches for wind turbines, PI, and observer-based state feedback controllers.

The aim of the paper is not focused on the design of the control system (already published in Do et al[19]). In addition to our previous work in this contribution, here, a new performance measure is introduced. In this paper, this performance measure is developed. Further, the proposed measure is used to assess the control performance of different approaches. As an example, those approaches already published in Do et al[19] are used for illustration. Furthermore, in addition to Do et al[19] and different results for wind speed region II, wind turbulence effects and control parameters effects also added for the application demonstration.

The paper is organized as follows: In Section 2, a brief description of two commonly used control approaches, PI and observer-based full-state controller, which are given as examples to illustrate the options of the new measure. The approaches are applied to a nonlinear 1.5-MW reference wind turbine model using FAST code.[20] In Section 3, classic performance measures and the new measure are presented. Illustration examples are provided in Section 4. Finally, conclusions drawn from the results are summarized.

2 | WIND TURBINE MODELING AND CONTROL

This section gives a brief overview about control model and methods used for comparison and illustration of the new measure. For simplicity, known PI and CPC observer-based full-state controllers are used for illustration. The PI controller is widely used in commercial wind turbines, while observer-based full-state approach is one of the most potential advanced control methods for wind turbines in practice. The wind turbine model and control approach used are similar to those in our previously published paper.[19]

FAST simulation code is used to obtain dynamic responses of different controllers and scenarios. The code can simulate important turbines' motions such as the translational (surge, sway, and heave) and rotational (roll, pitch, and yaw) motions of the support platform relative to the inertia frame, the tower motion, the yawing and nacelle motion, the generator motion, variable rotor speed and drive-shaft flexibility, the drivetrain motion, the blade flapwise tip motion for the first and second mode, the blade edgewise tip displacement for the first mode, and lastly, the rotor and tail furl. These motions or degree of freedoms (DOFs) can be disabled during the simulation to obtain less complex models.[20]

2.1 | Wind turbine model

A three-bladed upwind reference WindPACT 1.5-MW onshore wind turbine model developed by the National Renewable Energy Laboratory (NREL)[21] is considered as a reference system based on the FAST code. The model is built based on an actual commercial wind turbine and was used most extensively in the WindPACT program for studies of wind turbine technology innovations. The turbine's characteristics are outlined in Table 1. In this paper, all of the DOFs of the onshore wind turbine are enabled. However, only the generator speed, drivetrain torsional, first mode blade flapwise, and tower fore-aft DOFs are enabled to obtain a reduced order model for controller design.

The wind turbine dynamics is represented by the nonlinear model

$$M(q,u,t)\ddot{q} + f(q,\dot{q},u,d,t) = 0, \tag{1}$$

where M denotes the mass matrix containing inertia and mass components, f denotes the nonlinear "forcing function" vector, q, $\dot{q}$, and $\ddot{q}$ denote the DOFs displacements, velocities, and acceleration, respectively, u denotes the vector of control inputs, d denotes wind input, and t represents time.

The nonlinear wind turbine model is linearized about a given steady-state operating point to receive a linear model for controller design numerically using FAST. First, a constant speed wind is used as input for FAST linearization analysis; the blade pitch angles are kept constant. FAST automatically compute the periodic steady-state operation points and the corresponding linearized models. The periodic state-space matrices then are azimuth averaged to obtain the final model.[20] In this contribution, the nonlinear model (1) is linearized about the operating point in the above-rated wind speed region, with hub-height wind speed of v_{op} = 18 m/s, pitch angles of $\beta_{1op} = \beta_{2op} = \beta_{3op}$ = 20°, and nominal rotor speed of y_{op} = 20.463 rpm selected as steady-state operating points. In region II, the operation point is chosen as v_{op} = 8 m/s, $\beta_{1op} = \beta_{2op} = \beta_{3op}$ = 2.9°, and y_{op} = 14.8 rpm. The controller of each region is computed based on the corresponding linearized model.

TABLE 1 1.5-MW reference wind turbine specifications

Rated Rotor Speed	20.463 rpm
Hub height	84 m
Configuration	three blades, upwind
Cut_in, Rated, Cut_out wind speed	4, 12, 25 m/s
Gearbox ratio	87.965
Blade diameter	70 m
Rated power	1.5 MW
Blade pitch range	0°-90°

Generally, the variables of the linearized model are small variations about the selected steady-state operating point. The state-space representation of the related linearized model is given by

$$\begin{aligned}\dot{x}(t) &= Ax(t) + Bu(t) + B_d d(t)\\ y(t) &= Cx(t),\end{aligned} \tag{2}$$

where $x(t) = [\Delta q(t), \Delta\dot{q}(t)]^T$ denotes the state vector, A denotes the system matrix, B denotes the control input matrix, B_d denotes the disturbance input matrix, $u(t) = [\Delta\beta_1(t), \Delta\beta_2(t), \Delta\beta_3(t)]^T$ denotes the perturbed control input, $d(t) = \Delta v(t)$ denotes the perturbed hub height wind speed, and $y(t) = Cx(t)$ denotes the measured outputs.

The reduced model used for control design is obtained by enabling the rotor, generator, drivetrain, tower fore aft, and blade flapwise DOFs; a 11-state model with states representing blade, tower, drivetrain loads, and the generator speed is considered. The mechanical state vector x of the corresponding model is

$$x = \begin{bmatrix} \text{tower fore-aft displacement}\\ \text{drivetrain torsional displacement}\\ \text{blade 1 flap-wise displacement}\\ \text{blade 2 flap-wise displacement}\\ \text{blade 3 flap-wise displacement}\\ \text{generator speed}\\ \text{tower fore-aft velocity}\\ \text{drivetrain torsional velocity}\\ \text{blade 1 flap-wise velocity}\\ \text{blade 2 flap-wise velocity}\\ \text{blade 3 flap-wise velocity} \end{bmatrix}. \tag{3}$$

The measured outputs include generator speed, tower fore-aft displacement, and blade flapwise displacements that can be easily obtained from typical sensors of modern turbines.

The FAST code does not integrate pitch actuator dynamics; hence ,an additional actuator model is required. For simplicity and because of the larger bandwidth of the pitch actuator dynamics relative to the wind turbine dynamics, here, the actuator dynamics is considered as a first-order (PT1) linear model

$$\frac{\beta}{\beta_{com}} = \frac{1}{s\tau_\beta + 1}, \tag{4}$$

where β_{com} represents the desired pitch angle, β the actual pitch angle and τ_β the actuator lag time. The actuator model can be expressed in state space form

$$\dot{\beta} = -1/\tau_\beta \beta + 1/\tau_\beta \beta_{com}. \tag{5}$$

From (2) and (5), the extended wind turbine model including the pitch actuator dynamics,

$$\begin{bmatrix}\dot{x}\\ \dot{\beta}\end{bmatrix} = \begin{bmatrix} A & B\\ 0 & -1/\tau_\beta\end{bmatrix}\begin{bmatrix} x\\ \beta\end{bmatrix} + \begin{bmatrix} 0\\ 1/\tau_\beta\end{bmatrix} u + \begin{bmatrix} B_d\\ 0\end{bmatrix} d, \tag{6}$$

can be obtained, where u denotes β_{com} instead of β. In following sections, the extended model included that actuator dynamics is used instead of the original one.

2.2 | Baseline controller

For below-rated wind speed region (region II), the main goal is to maximize the power production. The pitch angle β is typically held constant at the optimal value β_{op}, the generator torque T_g is varied to control the rotor speed in order to maximize the power extracted. At fixed pitch angle, maximum aerodynamic efficiency is achieved at the optimal rotor speed Ω_{rop} or tip-speed ratio λ_{op}, which maximizes the power coefficient C_p. The typical generator torque controller is expressed as

$$T_g = K\Omega^2(t) = \frac{1}{2N_g}\rho\pi R^5 \frac{C_{p_{op}}(\beta_{op}, \lambda_{op})}{\lambda_{op}^3}\Omega_r^2(t), \tag{7}$$

where N_g denotes the gearbox ratio between generator and rotor speed, ρ denotes air density, R the rotor radius, and Ω_r denotes rotor speed.[22]

In high wind speed regime (region III) that is above-rated wind speed, the wind energy is beyond the extraction capacity of the turbines. The main goal in this region is to keep the turbines operate under the electrical and mechanical safety limits. Two typical strategies for region III wind turbines control are constant power and constant torque. In the constant power strategy, the generator power is kept constant by varying the generator torque inversely proportional to the generator speed.[23] In the second strategy, the generator torque is held constant, while the

rotor/generator speed is regulated to the desired rated value by modifying the blade pitch angles.[21] In this paper, the constant generator torque approach is used as an example; the generator speed is then controlled by a PI controller.

PI control approach is the most widely used method of commercial wind turbines control in region III. A PI controller formula can be written as

$$u(t) = K_p e(t) + K_i \int e(\tau) d\tau, \tag{8}$$

where K_p and K_i denote the coefficients for the proportional and integral terms respectively, $u(t)$ denotes the control variable that is the collective demanded pitch angle, and $e(t)$ denotes the difference between desired and measured rotor speed. The parameters K_p and K_i are defined by the method described in Wright and Fingersh[24] using the linear model (2).

2.3 | FSF controller

The baseline controller designs do not consider structural loads. To reduce loads while maximizing power production in partial load scheme and regulate the power in full load region, FSF controllers can be applied to add damping to blade and tower bending modes. Using the linear model (2), a linear quadratic regulator (LQR) is designed such that the objective function J_{LQR},

$$J_{LQR} = \int \left(x^T(t) Q x(t) + u^T(t) R u(t) \right) dt, \tag{9}$$

is minimized, where Q and R are state and control input weighting matrices, respectively. The weighting matrices provide a trade-off between state regulation and control efforts. A typical way to choose suitable weighting matrices is to keep R constant (let say $R = I$) and vary Q. To realize the objective of reducing structural load on blades and tower vibration, the elements of the Q weighting matrix related to blades and tower motions can be tuned. For each attempt, performance measures are applied and compared until the desired values are obtained.

The control variable $u(t)$ can be calculated as $u(t) = Gx(t)$, where $G = -R^{-1}B^T P$. The matrix P is obtained by solving the algebraic Riccati equation as

$$AP + PA^T + Q - PR^{-1}B^T P = 0. \tag{10}$$

The controller requires the feedback state values; however, some of the states are not always available or expensive to measure. In this contribution, the estimated state values $\hat{x}(t)$ provided by a PI observer (PIO) described in the next section are used as feedback variables.

2.4 | PI observer

Based on a system model, observers can reconstruct the unmeasured states from measurements of outputs. Classical observers such as Luenberger observer and Kalman filter are not directly applicable to nonlinear systems as wind turbines.

A PIO can be applied to estimate the system states, while nonlinearities as unknown inputs are acting to the system. Nonlinear model (1) can be rewritten in the form of combined linear and nonlinear parts as

$$\begin{aligned} \dot{x}(t) &= Ax(t) + Bu(t) + Nf(x,t) \\ y(t) &= Cx(t). \end{aligned} \tag{11}$$

where, $f(x,t) \in \mathbb{R}^r$ denotes the nonlinearities, unmodeled dynamics, and unknown inputs assumed as additive inputs, $x(t) \in \mathbb{R}^n$ denotes the state vector, $u(t) \in \mathbb{R}^l$ denotes the input vector, and $y(t) \in \mathbb{R}^m$ denotes the measured output vector. The information about the dynamics of $f(x,t)$ is assumed as unknown. The matrix N denotes the location of unknown inputs acting to the system and is assumed as known.

The aim is based on the given information of the system model, the matrices $A \in \mathbb{R}^{n\times n}$, $B \in \mathbb{R}^{n\times l}$, $C \in \mathbb{R}^{n\times n}$, and $N \in \mathbb{R}^{n\times r}$, to estimate the system states $x(t)$ as $\hat{x}(t)$ and the effects of the nonlinearity and unmodeled dynamics $f(t)$ as $\hat{f}(t)$ as unknown inputs. The system is assumed as controllable and observable for the existence of the controller and observer. The condition is satisfied by choosing control variables and measured outputs.[25] The basic idea is to extend the system states with an additional state to express the nonlinearity and unmodeled dynamics. Without exact knowledge about the dynamics of unknown input $f(t)$ and assuming that $f(t)$ is varying slowly so that the dynamics can be assumed as piecewise constant, the dynamics $f(t)$ is expressed as

$$\dot{f}(t) = Df(t) \leq \epsilon, \tag{12}$$

where ϵ denotes a slow and bonded change rate and is a very small number. If the unknown dynamics $f(t)$ is assumed as piecewise constant, $D = 0$.[26]

The extended system is described by

$$\begin{aligned} \begin{bmatrix} \dot{x}(t) \\ \dot{f}(t) \end{bmatrix} &= A_e \underbrace{\begin{bmatrix} A & N \\ 0 & 0 \end{bmatrix}}_{x_e} \underbrace{\begin{bmatrix} x(t) \\ f(t) \end{bmatrix}} + B_e \underbrace{\begin{bmatrix} B \\ 0 \end{bmatrix}} u(t) \\ y(t) &= C_e \underbrace{\begin{bmatrix} C & 0 \end{bmatrix}} \begin{bmatrix} x(t) \\ f(t) \end{bmatrix}. \end{aligned} \tag{13}$$

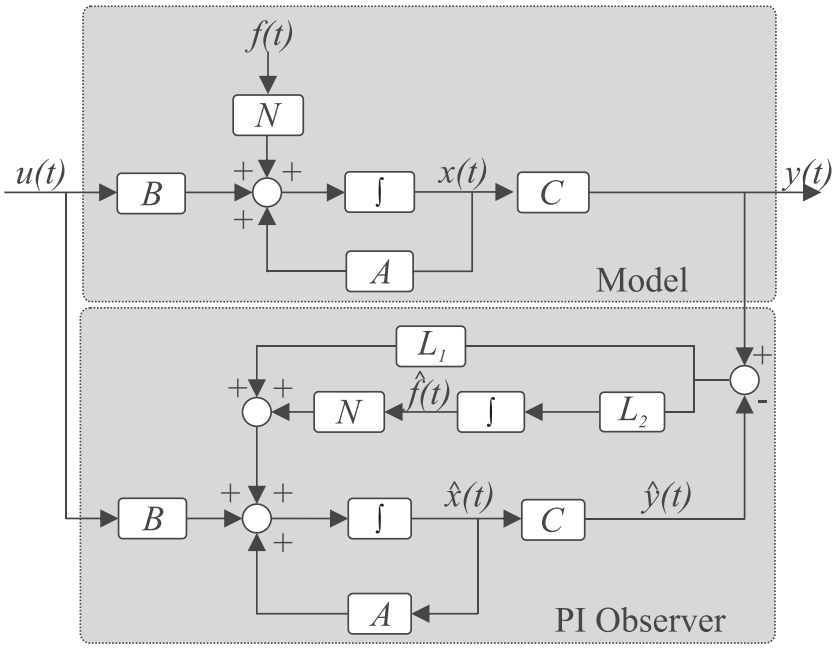

FIGURE 1 Proportional-integral (PI) observer

Assuming observability of A_e and C_e, the states $x(t)$ and the unknown $f(t)$ in (11) can be estimated as

$$\begin{bmatrix} \dot{\hat{x}}(t) \\ \dot{\hat{f}}(t) \end{bmatrix} = \begin{bmatrix} A & N \\ 0 & 0 \end{bmatrix} \begin{bmatrix} \hat{x}(t) \\ \hat{f}(t) \end{bmatrix} + \begin{bmatrix} B \\ 0 \end{bmatrix} u(t) + \begin{bmatrix} L_1 \\ L_2 \end{bmatrix} (y(t) - \hat{y}(t)). \tag{14}$$

This extended system can also be interpreted by adding an integral part to a classical Luenberger observer shown in Figure 1 where L_1 is original Luenberger gain and L_2 is additional integral gain of the observer.

Based on (13) and (14), considering the estimation errors as $e(t) = \hat{x}(t) - x(t)$ and $f_e(t) = \hat{f}(t) - f(x, t)$, the error dynamics of the extended system becomes

$$\begin{bmatrix} \dot{e}(t) \\ f_e(t) \end{bmatrix} = \underbrace{\begin{bmatrix} A - L_1 C & N \\ -L_2 C & 0 \end{bmatrix}}_{A_{e,obs}} \begin{bmatrix} \hat{e}(t) \\ f_e(t) \end{bmatrix} + \begin{bmatrix} L_1 \\ L_2 \end{bmatrix} (y(t) - \hat{y}(t)). \tag{15}$$

For a suitable observer design, the feedback matrix L has to be chosen in such a way that the estimation errors tend to zero ($e(t) \to 0, f_e(t) \to 0$). The error dynamics is affected by the term $f(x, t)$. The feedback matrices L_1 and L_2 are required to stabilize the extended system described by the matrix $A_{e,obs}$ and to minimize the influence from the unknown inputs $f(t)$ to the estimations $e(t)$ and $f_e(t)$. The two requirements

- $Re(\lambda_i) < 0$, for all the eigenvalues of matrix $A_{e,obs}$, and
- $\|L_2\|_F \gg \|L_1\|_F$,

for the PIO gain matrices design have to be fulfilled, where $\|.\|_F$ denotes the Frobenius norm.

These requirements can be realized by using LQR method with suitable weighting matrices

$$Q_{obs} = \begin{bmatrix} I_n & 0 \\ 0 & qI_r \end{bmatrix}, R_{obs} = I_m, \tag{16}$$

with q as scalar design parameter so that $\|L_2\|_F \gg \|L_1\|_F$ with $q \gg 1$ expressing "high-gain."[27]

The overall PIO-based FSF control system for wind turbines is shown in Figure 2. The wind turbine is assumed to operate only at regions II or III. The transition region (region $2_{1/2}$) is not considered in this paper. The region II control system includes a baseline torque controller described in Section 2.2 and a PIO-based FSF controller. The FSF controller adjusts the blade pitch angles around the optimal value to provide additional damping to the structural load variation modes. In region III, the torque is kept constant at rated value; the objectives of the FSF controller in this region are to regulate the rotor/generator speed and reduce structural variations. Note that the two FSF controllers have different parameters calculated from linearized models described in Section 2.1.

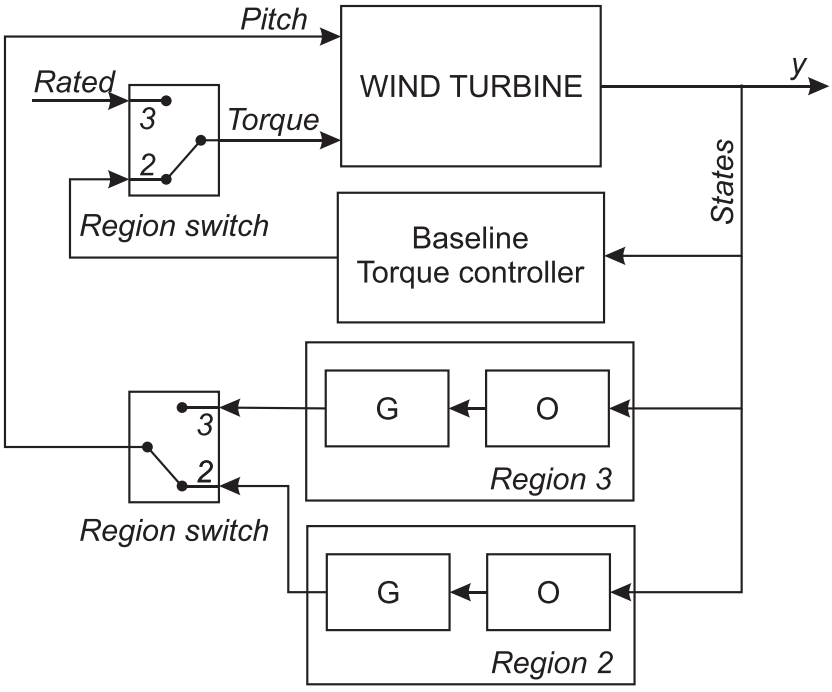

FIGURE 2 Wind turbine control system

3 | PERFORMANCE MEASURES

3.1 | Power spectral density

PSD analysis is a type of frequency-domain analysis methods describing the distribution of power or the strength of variation into frequency components.[17] In other words, PSD shows the strength of variation at certain frequencies.

For load analysis of wind turbines, PSDs are often used to determine blade and tower variation power at rotor frequency (1P, one-per-revolution) and multiples of rotor frequency (2P, 3P, and so on), which correspond to structural loads.

To obtain PSDs, time series data of tower and blades variation are transformed to frequency domain by truncated Fourier transform over a finite interval T as

$$x(\omega) = \frac{1}{\sqrt{T}} \int_0^T x(t) e^{-i\omega t} dt. \tag{17}$$

The PSD or power spectrum is calculated as

$$P(\omega) = \lim_{T \to \infty} E\left[|x(\omega)|^2\right], \tag{18}$$

where E denotes the expected value.[28]

3.2 | Damage equivalent load

Wind turbine components are subjected to variable mechanical stresses because of variability of wind speed leading to gradual degradation of individual components. To assess the structural load, the fatigue load is widely used as describing variable. In material science, fatigue is the weakening of a material because of cyclical applied loads that are beyond certain thresholds.[29]

Miner's rule[30] is often used to calculate cumulative damage for failures caused by fatigue. Assuming there are k different load amplitude levels, namely, $S_i, (1 \leq i \leq k)$, each level S_i contributes n_i cycles, and the number of cycles to failure at the stress level S_i is N_i. The number of cycles to failure N_i is defined by a stress-cycle (S-N) curve. The S-N curves are derived from experiment on samples of the material. The damage accumulation D_{ac} can be expressed as

$$D_{ac} = \sum_{i=1}^{k} D_i = \sum_{i=1}^{k} \frac{n_i(S_i)}{N_i(S_i)}, \tag{19}$$

with D_i as damage increment and D_{ac} as accumulated damage over actual lifespan. In general, when the damage accumulation D_{ac} reaches a defined limit ≥ 1, the system is considered as failed.

For arbitrary stresses, rainflow-counting (RFC) algorithm is used[31] to transform a spectrum of varying stress levels to a set of simple load levels allowing the application of Miner's rule.

To justify the damage in a period of time, DEL, which is a constant amplitude fatigue load defining the equivalent damage as the variable spectrum of loads,[18] can be calculated as

$$DEL = \left(\frac{\sum_i n_i S_i^m}{N} \right)^{\frac{1}{m}}, \tag{20}$$

where N denotes total equivalent fatigue counts, m the Wöhler exponent, and both are defined by experiments.

3.3 | New covariance distribution diagram measures

Existing measures for structural loads mentioned above only consider loads without referring to the relationship between loads and other control performance aspects such as the power regulation or the power extracted. To illustrate exactly this relationship, this paper proposed to place structural loads and generator power together in a covariance distribution diagram (Figure 3) as a base to form new measures.

For the uniform between regions II and III, the power regulation is use to represent the speed regulation, since the power is proportional to the speed when the torque is constant. In Figure 3, for a given load profile, each point represents the instantaneous values at a sample time of the bending moment of the tower (structure load) and the generated power related to a certain wind speed applying a specific control structure and parameter set combination. Thus, for given wind profile and a control system, an unique distribution can be obtained. The behaviors can be clearly distinguished and characterized by the area, density, and 2D width of related distributions (here, blue: FSF; red: PI controller).

To describe the related characteristics of the controllers more clearly, the covariance matrix of the relevant structural loads damage data D and generator power data P has to be calculated. Based on the covariance matrix, ellipse iso-contours are determined for controllers. Each ellipse is characterized by the center point m, the angles between the ellipse axes and the coordinate axes α, and the widths in both directions σ_x and σ_y. These variables can be used as performance measures, namely, CS_x (CS is the acronym for controller sensitivity), for wind turbine control system. The ellipse then is scaled by a factor determined by the chi-square probabilities table (24). The higher scale factor, the bigger ellipse containing more data points. In this paper, the scale factor is chosen to defining the ellipse containing 95% of all data (Figure 4).

The center points are determined by the average value of the load variations m_x (CS_3) and the generated power m_y (CS_4). The average load m_x is expected to be low. The higher m_y is better in wind speed region II since it indicates that more power is produced. However, in wind speed region III, the control goal is to keep generated power constant at rated value, so m_y is expected to be close to the set point.

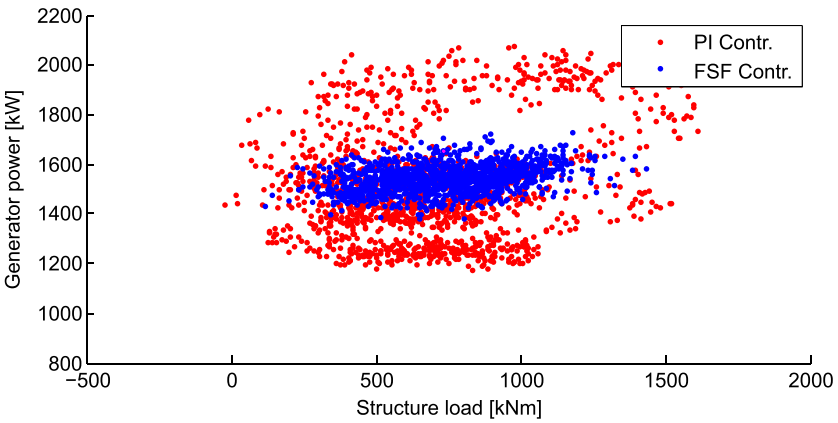

FIGURE 3 Comparison of load and power contributions (red: proportional-integral [PI], blue: full-state feedback [FSF] controller) [Colour figure can be viewed at wileyonlinelibrary.com]

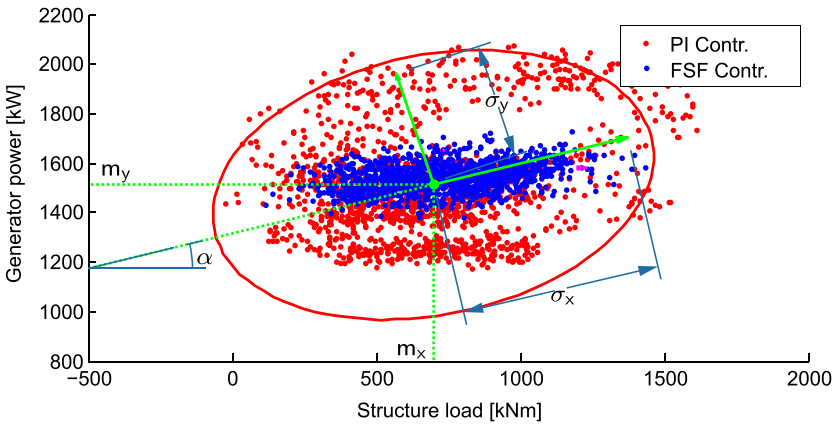

FIGURE 4 Illustration of the introduced measures CS_{1-5} applied to the result of PI controller. FSF, full-state feedback; PI, proportional-integral [Colour figure can be viewed at wileyonlinelibrary.com]

The angle α ($0 \leq \alpha \leq 90$) denotes the relationship between the loads and power; if the ellipse axes and the coordinate axes are aligned or the angle α equals to zero or 90°, the structural loads and generated power are uncorrelated. To illustrate the correlation level of the data, the newly measure CS_5 can be defined as

$$CS_5 = min(\alpha, 90 - \alpha). \tag{21}$$

Higher value of CS_5 defines, the higher power production will be connected with higher structural loads, so CS_5 is considered as a measure for the sensitivity of controllers (controller sensitivity - CS). The lower the value of CS_5 is, the better due to the related controller introduces lower additional structural loads; it can produce more power without increasing the loads.

The magnitudes σ of the ellipse axes define the variance of the data. The value of σ_x (CS_1) represents the strength of structural load variation, so the control goal for both wind speed regions is to keep σ_x as small as possible. In wind speed region II, power production related to σ_y (CS_2) and m_y (CS_4), higher σ_y and m_y means more power is produced. Typical control strategy for region II is using an additional loads reduction control loop with the baseline controller. The loads reduction controller only modifies the pitch angles around the optimal value to mitigate loads, so the mean generated power m_y is nearly the same as the baseline case (see Section 4.2). On the other hand, in wind speed region III, generated power is regulated to rated value, so σ_y need to be small in this region.

Table 2 summarizes proposed measures. The list of proposed measures is given in the first column with the corresponding variables given in the second column. The next two columns represent the application of proposed measures in regions II and III. In each region, the '+' sign denotes the higher of the corresponding measure, the better the performance. The "−" sign denotes the lower value of the measure is better.

Based on the ellipses representing the results of each controller, control performance information include structural load levels, generator power, and the relationship between loads and power, which is extracted and compared. This allows to justify the effectiveness of different control approaches, as well as to give criteria for tuning the control parameters.

The covariance of the two variable vectors X and Y are defined as

$$cv(X, Y) = \frac{1}{N-1}\sum_{i=1}^{N}(X_i - m_x) * (Y_i - m_y), \tag{22}$$

where m_x and m_y denote the mean of X and Y and $*$ denotes the complex conjugate. The covariance matrix of X and Y is calculated as

$$C = \begin{bmatrix} cv(X,X) & cv(X,Y) \\ cv(Y,X) & cv(Y,Y) \end{bmatrix}. \tag{23}$$

Using the covariance matrix, the ellipse equation is formulated as

$$\left(\frac{x}{\sigma_x}\right)^2 + \left(\frac{y}{\sigma_y}\right)^2 = s, \tag{24}$$

where s denotes the scale factor of the ellipse determined by the chi-square probabilities table (95% confidence level corresponds to $s = 5.99$) and σ_x and σ_y are standard deviations of structural load and generator power data, which are related to the eigenvalues λ of the covariance matrix C as

$$CS_{1/2} = \sigma_i = \sqrt{\lambda_i}, det(C - \lambda I) = 0. \tag{25}$$

The ellipse is centered at the mean values of data (m_x, m_y) and rotated around the X-axis an angle α equal to the angle of the largest eigenvector v_{max} of C towards the X-axis

$$\alpha = arctan\frac{v_{max}(y)}{v_{max}(x)}. \tag{26}$$

TABLE 2 New measures summary

CS measures	Variables	Region II	Region III
CS_1	σ_x	−	−
CS_2	σ_y	+	−
CS_3	m_x	−	−
CS_4	m_y	+	NA
CS_5	α	−	−

Note. +, Higher is better; −, lower is better; NA, not defined. Abbreviation: CS, controller sensitivity.

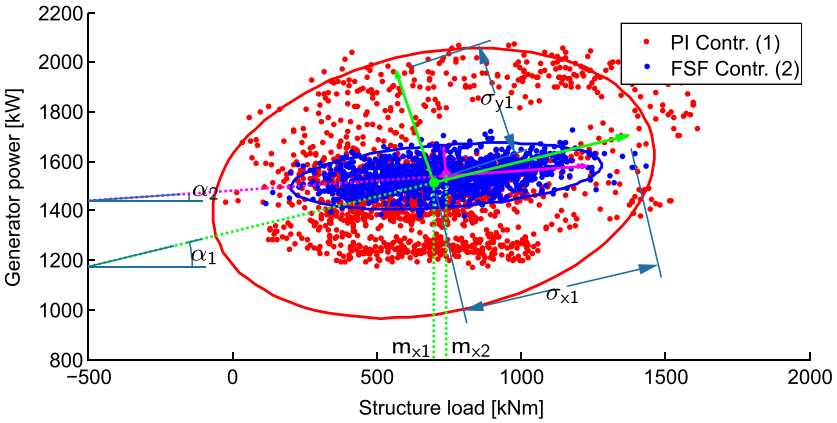

FIGURE 5 Illustration of the introduced measures CS_{1-5} applied to the results of two controllers (red: proportional-integral [PI], blue: full-state feedback [FSF]) [Colour figure can be viewed at wileyonlinelibrary.com]

TABLE 3 PI and FSF controller comparison

CS measures	CS_1	CS_2	CS_3	CS_4	CS_5
Variables	σ_x	σ_y	m_x	m_y	α
PI (1)	328	218	697	1512	17
FSF (2)	238	46	744	1540	5

Note: Green shade refers to better results.

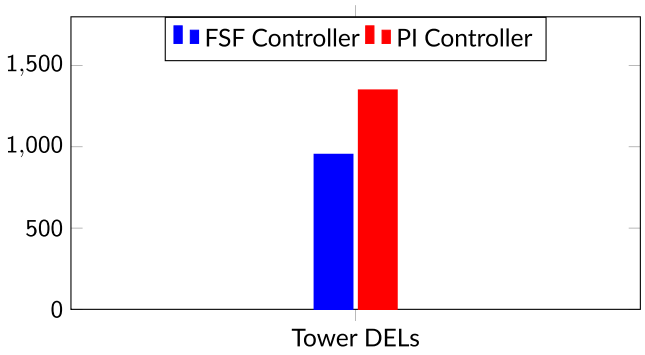

FIGURE 6 Damage equivalent loads. FSF, full-state feedback; PI, proportional-integral [Colour figure can be viewed at wileyonlinelibrary.com]

As example in Figure 5 and Table 3, the results comparison of the PI and FSF controllers for wind speed region III are given. In wind speed region III, the rotor speed is regulated to the design-rated value to avoid too high mechanical stresses by governing the blade angles, while the generator torque is held constant. It can be obtained that FSF controller has much better speed regulation performance than classical PI controller (79% smaller CS_2 or generator speed variation). In addition, by applying FSF controller, the structural loads (tower bending moment) that the turbine has to withstand also reduce by 27% indicated by reduction in CS_1; the correlation between structural loads and generated power is also reduced (smaller orientation angle CS_5).

For comparison with the new measures, the tower DELs of both controllers are calculated (Figure 6) using Mlife.[18] The results show that by using the FSF controller, the tower DEL reduces by 29%, which is a good agreement with the results of the new measures. However, in the DEL metric, only structural load is considered; no information regarding the speed regulation performance and the correlation is provided.

It can be easily observed from the new measures graphically represented in Figure 4 that the FSF controller has advantages over the PI controller in the both objectives, rotor speed regulation, and structural loads mitigation. In the new measures, CS_{1-4} defines a generalized representation of commonly used load amplitude measure for load analysis; CS_5 is completely new and introduces an additional measure for controller assessment and design. All new measures are visualized graphically in one figure; it is convenient for designers to assess and compare the performances of each controller.

4 | ILLUSTRATIVE EXAMPLES

The proposed measures are applied to compare PI and FSF controller in both wind speed regions II and III to illustrate the ability of performance evaluation using the measures introduced. The normal power production design load case DLC 1.2 for fatigue according to the IEC 61400-1 standard is used.[32] The results are obtained using FAST code with the wind turbine model and control methods described in Section 2.

Turbulence wind profiles used for simulation are generated using IEC von Karman wind turbulence model by TurbSim.[33] The wind has a mean value of 8 m/s for region II and 18 m/s for region III simulation; the linear vertical wind shear power law exponent is 0.2. The turbulence intensity of the wind is chosen as 12% corresponding to standard IEC category C. Three different random seeds are used for each wind profile to analyze the fatigue loads that are the tower bending moments of the turbine.

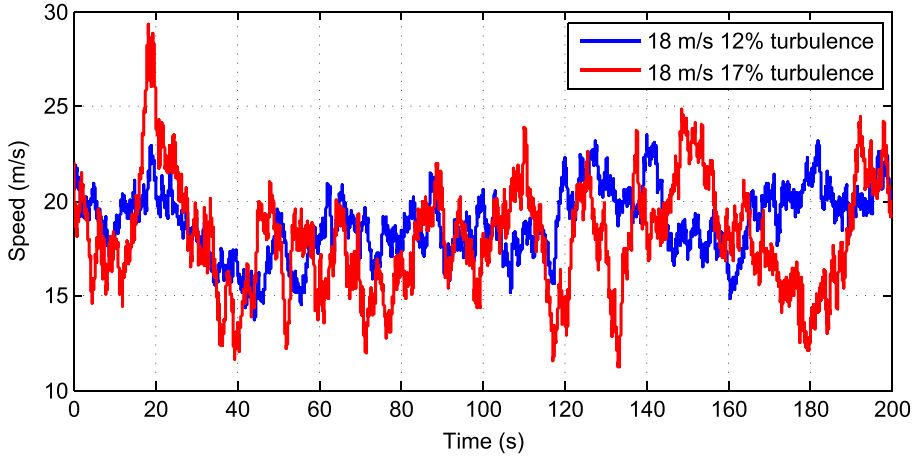

FIGURE 7 Hub height wind profiles with the same mean speed and different turbulence levels [Colour figure can be viewed at wileyonlinelibrary.com]

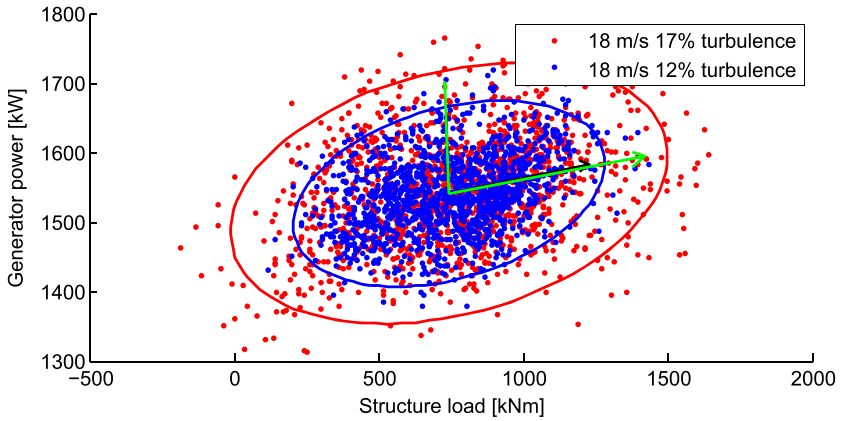

FIGURE 8 Illustration of the effects of the wind turbulence level on control performances using new measures [Colour figure can be viewed at wileyonlinelibrary.com]

4.1 | Wind turbulence level effects

To study the effects of wind turbulence level on the control performances using the new measures, two wind profiles with different turbulence intensity of 12% (IEC type C) and 17% (IEC type A) are used in comparison with the same controller (Figure 7).

The results are obtained for both wind profiles with FSF controller. From Figure 8, it can be observed that the representative ellipses have identical center points and angles shown by the same value of CS_3, CS_4, and CS_5. This means the change in the turbulence level of wind profiles does not affect the correlation between structural loads and generated power when using the same controller. The variation in generated power and loads indicated by CS_2 and CS_1, on the other hand, increase about 25% when the wind turbulence level raises from 12% to 17%. Each controller is characterized by the relation between loads and power produced or the angles between corresponding ellipse axes and coordinate axes. The control performance levels depend on both control approach and wind characteristics.

4.2 | Wind speed region II

In wind speed region II that is below rated speed, the control objectives are to maximize extracted power from the wind while keeping the structural loads smallest possible. Typically, the control design goals are realized by a torque controller to govern the rotor speed to reach optimal value depending on wind speed. The blade angles are kept constant at a predefined optimal value. To better mitigate structural loads, a FSF controller is used combined with existing torque controller to add damping into the blades and tower bending modes. The additive controller modifies the blade angles around optimal value to reduce the blades and tower variations. The modification may affect the overall optimum tip-speed ratio, thus reducing the extracted power; however, the mean values of loads (m_x) and power (m_y) are remained the same. This trade-off is shown in Figure 9. The magnitude of the ellipse in vertical direction represents variations of generator power, and in horizontal direction, represents those related to structural loads. From the simulation results in Figure 9, a reduction of 32% in structural load (CS_1) exchange for 10% decrease in power production (CS_2) can be observed. It is also can be detected that the produced loads and power are uncorrelated in this scenario for both control approaches because of CS_5 equal to zero.

4.3 | Wind speed region III

In wind speed region III that is above-rated speed, the rotor speed is regulated to the design rated value by the PI controller to avoid mechanical stress larger than that designed by governing the blade angles, while the generator torque is held constant. In this situation, FSF controller has

much better speed regulation performance than classical PI controller (80% smaller CS_2 rotor speed variation) (Figure 10). In addition, by applying FSF controller, the structural loads that the turbine has to withstand are also reduce by 27% indicated by reduction in CS_1.

4.4 | Controller parameter design

For an illustration of using the new measures for designing controller in wind speed region III, the weighting matrix Q of the FSF controller is tuned and compared to determine the best parameters. For example, three combinations of controller parameters are used. The element of the weighting

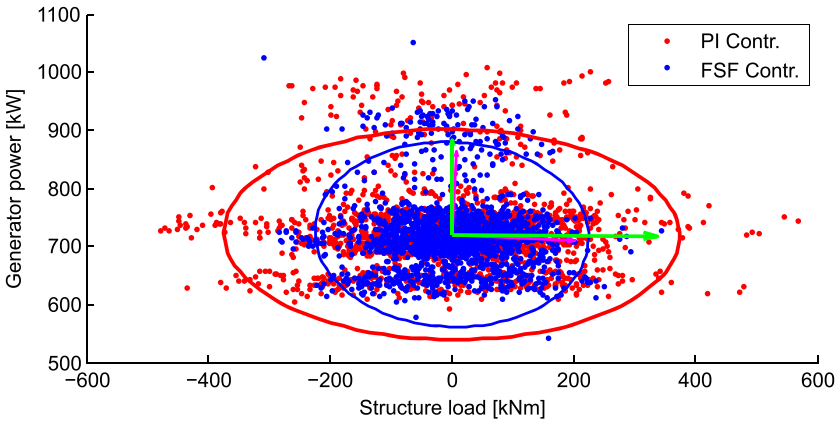

FIGURE 9 Comparison performances of two controllers in wind speed region II using new measures. FSF, full-state feedback; PI, proportional-integral [Colour figure can be viewed at wileyonlinelibrary.com]

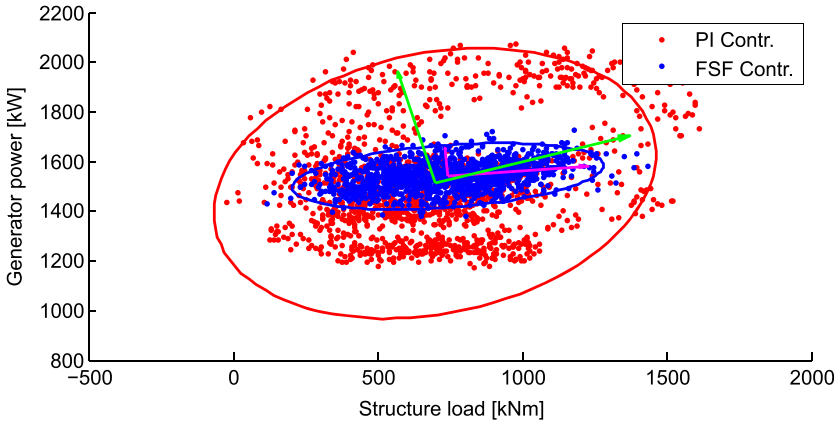

FIGURE 10 Comparison performances of two controllers in wind speed region III using new measures. FSF, full-state feedback; PI, proportional-integral [Colour figure can be viewed at wileyonlinelibrary.com]

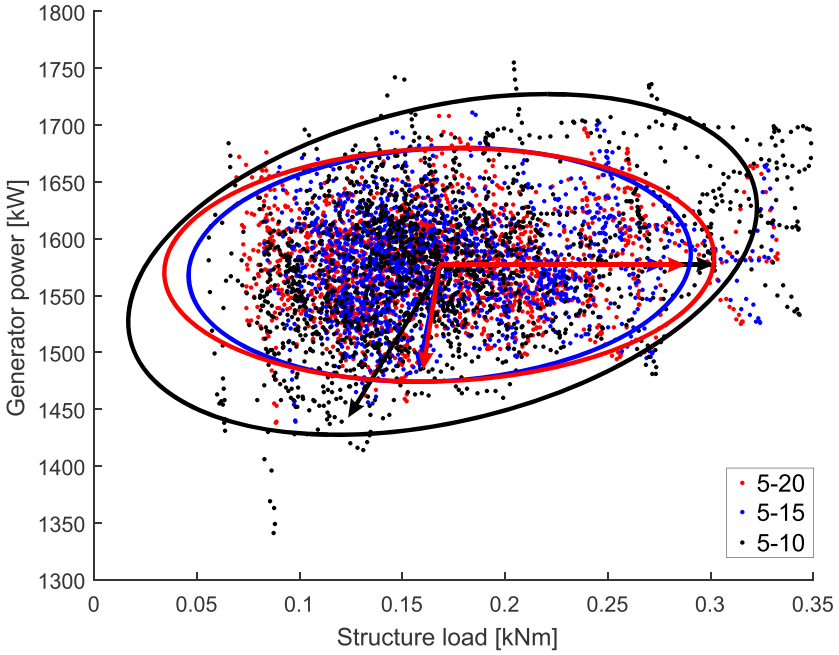

FIGURE 11 Comparison results of a FSF controller with different weightings (5-20, 5-15, and 5-10) using new measures. FSF, full-state feedback [Colour figure can be viewed at wileyonlinelibrary.com]

CS measures	CS_1	CS_2	CS_3	CS_4	CS_5
Variables	σ_x	σ_y	m_x	m_y	α
5-20	0.134	102.7	0.168	1577	1.57
5-15	0.122	102.8	0.168	1577	1.57
5-10	0.144	149.9	0.169	1577	1.57

Abbreviations: CS, controller sensitivity; FSF, full-state feedback.

TABLE 4 Comparison results of a FSF controller with different weightings (5-20, 5-15, and 5-10) using new measures

matrix Q corresponding to the rotor speed regulation performance is chosen constantly at 5; the element corresponding to structural load (in this case is blade bending moments) is varied at increasing values 10, 15, and 20. So three combinations of weighting are 5 to 10, 5 to 15, and 5 to 20.

The results are shown in Figure 11 and Table 4; it can be seen that CS_3, CS_4, and CS_5 do not change when varying Q, which means that the correlation between structural loads and power production remain the same for all combinations. However, CS_1 and CS_2, representing structural load mitigation and rotor speed regulation performances, are changing depending on the value of the weighting matrix Q. By increasing the coefficient from 10 to 15, CS_1 and CS_2 decrease; the control performance for both criteria are improved. When continuously increasing the coefficient from 15 to 20, CS_1 increases; the load mitigation performance is reduced, while CS_2 nearly unchanged. It can bee observed from the new measures that the best parameter combination for the FSF controller is 5 to 15 in this situation.

5 | CONCLUSIONS

In this contribution, new measures are introduced to characterize and, therefore, also to compare control approaches applied to wind turbine control systems. The measures are able to describe the different and conflicting control goals of wind turbines by graphical and numerical representations. Five measures are introduced: CS_1 denotes the strength of force variation representing structural loads; CS_2 denotes power variation representing power production in region II and the accuracy of power regulation in region III; CS_3 and CS_4 denote the mean values of loads and generated power; and finally ,CS_5 denotes the relationship between loads and power as a measure for the sensitivity of controllers. All measures are visualized graphically in one figure providing quick evaluation and comparison of control performances.

As illustrative examples, two different controllers are applied to express the measure options introduced. Now, for the first time, it is possible to qualify control approaches regarding both conflict goals structural load reduction and control performance improvement. The measures can help to evaluate different performance dimensions of controllers to analyze the effects of various aspects to the system behaviors and give new design criteria for tuning controllers.

ACKNOWLEDGEMENT

The research reported in this paper is partly supported by the Vietnam International Education Development (VIED) scholarship received by the first author for his Dr.-Ing. study at the Chair of Dynamics and Control, UDE, Germany.

ORCID

M. Hung Do https://orcid.org/0000-0002-8485-4139

REFERENCES

1. Hamdi H, Mrad C, Nasri R. Effects of gyroscopic coupling on the dynamics of a wind turbine blade with horizontal axis. In: T Fakhfakh, W Bartelmus, F Chaari, R Zimroz, M Haddar, eds. *Condition Monitoring of Machinery in Non-Stationary Operations*. Berlin, Heidelberg: Springer; 2012:159-174. https://doi.org/10.1007/978-3-642-28768-8_17
2. Laks JH, Pao LY, Wright AD. Control of wind turbines: past, present, and future. In: IEEE American Control Conference, 2009. ACC'09; 2009:2096-2103. https://doi.org/10.1109/ACC.2009.5160590
3. Bossanyi EA. Individual blade pitch control for load reduction. *Wind Energy: An Int J Prog Appl Wind Power Convers Technol*. 2003b;6(2):119-128. https://doi.org/10.1002/we.76
4. Duckwitz D, Shan M. Active tower damping and pitch balancing–design, simulation and field test. In: Conference: 4. Science of Making Torque from Wind Conference, Oldenburg (Germany), 9-11 Oct 2012; Other Information: Country of input: International Atomic Energy Agency (IAEA), Vol. 555; 2014:11. https://doi.org/10.1088/1742-6596/555/1/012030
5. Pintea A, Christov N, Popescu D, Borne P. LQG control of horizontal wind turbines for blades and tower loads alleviation. *IFAC Proc Vol*. 2011;44(1):1721-1726. https://doi.org/10.3182/20110828-6-it-1002.01231
6. Imran RM, Hussain DMA, Chen Z. LQG controller design for pitch regulated variable speed wind turbine; 2014:101-105. https://doi.org/10.1109/energycon.2014.6850413
7. Evans MA, Cannon M, Kouvaritakis B. Robust MPC tower damping for variable speed wind turbines. *IEEE Trans Control Syst Technol*. 2014;23(1):290-296. https://doi.org/10.1109/tcst.2014.2310513
8. Mirzaei M, Soltani M, Poulsen NK, Niemann HH. An MPC approach to individual pitch control of wind turbines using uncertain LIDAR measurements. In: European Control Conference (ECC). IEEE; 2013:490-495. https://doi.org/10.23919/ecc.2013.6669729

9. Wang N, Wright AD, Balas MJ. Disturbance accommodating control design for wind turbines using solvability conditions. *J Dyn Syst Meas Control*. 2017;139(4):041007. https://doi.org/10.1115/1.4035097
10. De Corcuera AD, Pujana-Arrese A, Ezquerra JM, Segurola E, Landaluze J. H∞ based control for load mitigation in wind turbines. *Energies*. 2012;5(4):938-967. https://doi.org/10.3390/en5040938
11. Yuan Y, Tang J. Adaptive pitch control of wind turbine for load mitigation under structural uncertainties. *Renew Energy*. 2017;105:483-494. https://doi.org/10.1016/j.renene.2016.12.068
12. Ma Z, Shaltout ML, Chen D. An adaptive wind turbine controller considering both the system performance and fatigue loading. *J Dyn Syst Meas Control*. 2015;137(11):111007. https://doi.org/10.1115/1.4031045
13. Xiao Y, Li Y, Rotea MA. Multi-objective extremum seeking control for enhancement of wind turbine power capture with load reduction. *J Phys Conf Ser*. 2016;753. https://doi.org/10.1088/1742-6596/753/5/052025
14. Bossanyi EA. Further load reductions with individual pitch control. *Wind Energy: An Int J for Prog Appl Wind Power Convers Technol*. 2005;8(4):481-485. https://doi.org/10.1002/we.166
15. Bir G. Multi-blade coordinate transformation and its application to wind turbine analysis. In: 46th AIAA aerospace sciences meeting and exhibit; 2008:1300. https://doi.org/10.2514/6.2008-1300
16. Bossanyi E, Fleming P, Wright A. Field test results with individual pitch control on the NREL CART3 wind turbine. In: In: 50th AIAA Aerospace Sciences Meeting Including the New Horizons Forum and Aerospace Exposition, Nashville, TN, January; 2012:9-12. https://doi.org/10.2514/6.2012-1019
17. Norton MP, Karczub DG. *Fundamentals of Noise and Vibration Analysis for Engineers*. Cambridge: Cambridge University Press; 2003. https://doi.org/10.1017/CBO9781139163927
18. Hayman G. Mlife theory manual for version 1.00. https://nwtc.nrel.gov/system/files/MLife_Theory.pdf; 2012.
19. Do MH, Njiri JG, Söffker D. Structural load mitigation control for nonlinear wind turbines with unmodeled dynamics. In: IEEE, Annual American Control Conference (ACC); 2018:3466-3471. https://doi.org/10.23919/acc.2018.8431121
20. Jonkman JM, Buhl Jr ML. FAST User's Guide-Updated August 2005. *tech. rep*, National Renewable Energy Lab. (NREL), Golden, CO (United States); 2005. https://www.nrel.gov/docs/fy06osti/38230.pdf
21. Malcolm DJ, Hansen AC. WindPACT Turbine Rotor Design Study: June 2000–June 2002 (Revised). *tech. rep.*, National Renewable Energy Lab. (NREL), Golden, CO (United States); 2006. https://www.nrel.gov/docs/fy06osti/32495.pdf
22. Bossanyi EA. Wind turbine control for load reduction. *Wind energy*. 2003a;6(3):229-244. https://doi.org/10.1002/we.95
23. Jonkman J, Butterfield S, Musial W, Scott G. Definition of a 5-MW reference wind turbine for offshore system development. *tech. rep.*, National Renewable Energy Lab.(NREL), Golden, CO (United States); 2009.
24. Wright AD, Fingersh LJ. Advanced control design for wind turbines; Part I: control design, implementation, and initial tests. *tech. rep.*, National Renewable Energy Lab. (NREL), Golden, CO (United States); 2008. https://www.nrel.gov/docs/fy08osti/42437.pdf
25. Wright AD. Modern control design for flexible wind turbines. *tech. rep.*, National Renewable Energy Lab., Golden, CO (US); 2004.
26. Söffker D, Yu T, Müller PC. State estimation of dynamical systems with nonlinearities by using proportional-integral observer. *Int J Syst Sci*. 1995;26:1571-1582. https://doi.org/10.1080/00207729508929120
27. Liu Y, Söffker D. Robust control approach for input-output linearizable nonlinear systems using high-gain disturbance observer. *Int J Robust and Nonlinear Control*. 2014;24:1099-1239. https://doi.org/10.1002/rnc.2889
28. Grimmett G, Stirzaker D. *Probability and Random Processes*. Oxford: Oxford University Press; 2001. https://doi.org/10.1016/C2010-0-67611-5
29. Schütz W. A history of fatigue. *Eng fract mechan*. 1996;54(2):263-300. https://doi.org/10.1016/0013-7944(95)00178-6
30. Miner MA. Cumulative damage in fatigue. *J Appl Mech*. 1945;12(3):A159-A164.
31. Matsuishi M, Endo T. Fatigue of metals subjected to varying stress. *Japan Soc Mechan Eng, Fukuoka, Japan*. 1968;68(2):37-40.
32. IEC 61400-1. Wind turbines part 1: design requirements. International Electrotechnical Commission; 2005.
33. Jonkman BJ, Buhl Jr ML. TurbSim user's guide. National Renewable Energy Laboratory, https://nwtc.nrel.gov/system/files/TurbSim.pdf; 2009.

How to cite this article: Do MH, Njiri JG, Söffker D. Structural load mitigation control for wind turbines: A new performance measure. *Wind Energy*. 2020;23:1085–1098. https://doi.org/10.1002/we.2475